Journal of Solid Mechanics Vol. 15, No. 1 (2023) pp. 109-119
DOI: 10.22034/jsm.2022.1958120.1741

Research Paper

Investigation of Oblique Blast Loading on Trapezoidal Corrugated Core Sandwich Panels; Experimental and Numerical Study

H. Mohammadi Hooyeh, A. Naddaf Oskouei *, T. Mirzababaie Mostofi , Kh. Vahedi

Department of Solid Mechanics, Faculty of Mechanical Engineering, University of Eyvanekey, Garmsar, Iran

Received 8 November 2022; accepted 7 January 2023

ABSTRACT

In this work dynamic response of trapezoidal corrugated core sandwich panels subjected to oblique blast loading are studied both numerically and experimentally. The stand-off distance which has been determined from sandwich panel to center of the nearest face of the explosive cylinder is considered 300 *mm*. the experiments was performed at Four blast tube with different included angles of 0°, 15°, 30° and 45° respect to sandwich target plate. The results of numerical simulation, obtained using coupled Eulerian – Lagrangian (CEL) method at ABAQUS/Explicit software. Maximum mid- point deflection of back and front faces are compared with experiment results. The results show that with increasing angle of tilt of explosive the amount of back face deflection at angles of tilt 15°, 30° and 45° respect to the case of 0°, 4.68%, 5.86% and 9.77% decreases respectively. It is found that at the *z* direction, deformation profile is completely dome-shaped while the profile in the *x* direction is almost conical. The achieved results can be used to optimization designing of military vehicles and employed for civil infrastructure.

Keywords : Trapezoidal corrugated core; Sandwich panels; Oblique blast loading; Coupled Eulerian Lagrangian method.

1 INTRODUCTION

RECENTLY, designers by knowing the source of the explosion have been designing the walls of structures and the body of equipment's obliquely in front of the explosion. For example in order to carry out security missions and protect the occupants of military vehicles against mines, booby traps and roadside bombs, the personnel carrier is designed to be integrated and has a "V" shaped floor [1-5]. On the other hand, sandwich structures in many industries are used to protecting people and objects from explosion and impact. The sandwich structures employs for absorbs a large amount of energy from explosions and impacts and prevents damage to targets [6-12]. Accordingly, a large amount research studies have been carried out on the sandwich panels under direct blast loading and some investigation has been represented on the plate under oblique blast loading. At the following some of them are represented, respectively, Cai et al. [13] represented Multi-objective optimization for designing metallic corrugated

*Corresponding author. Tel.: +98 21 77107105; Fax: +98 21 77107105.
E-mail address: anadaf@eyc.ac.ir (A. Naddaf Oskouei)

core sandwich panels under air blast loading. They considered a finite element model for the represent of dynamic responses of trapezoidal corrugated core sandwich panel and validated by experiments. Zhang et al. [14] employed numerical simulation for analysis of corrugated core sandwich panels subject to near-field air blast loading. It is depicted that the profits of a sandwich panel over an equivalent weight solid plate to tolerate near-field air blast loading are more obvious at lower stand-off distance. Zhang et al. [15] performed the experiments on the laser-welded triangular corrugated core sandwich panels under blast loading. It was demonstrated that with the increase of both face sheet thickness and core web thickness of sandwich panel back face deflection decreased. It is also developed that an effective way to improve the blast resistance of panel could be increase the thickness of front face. Experimental analysis of foam filling on the dynamic response of metallic corrugated core sandwich panel subject to air blast loading illustrated by Cheng et al. [16] It is found from their results that foam filling is an effective method to enhance blast resistance of sandwich panels. At another study Zhang and his research group [17] investigated the effects of foam filling strategies of corrugated steel core sandwich panels by conducting air blast experiments. It is inspiring that the back side filling strategy is the least effective at decreasing the levels of fracture failure and plastic deformation. Dynamic and blast response of sandwich panels with layered graded aluminum honeycomb cores under blast loading has been carried out by Li et al. [18] it is found that the effect of back face sheet thickness on the deflection is less evident than that of the front face sheet. An experimental analysis for dynamic response of metallic trapezoidal corrugated-core sandwich panels under air blast loading represented by Zhang et al. [19] Zhou et al. [20] examined the blast response of sandwich panels with metallic face-sheets and polyvinyl chloride (PVC) foam ungraded/ graded cores. It is observed from their results that blast resistance of face sheet and core in graded panel with an optimal core gradation would bring profits, but also was confronted to face the risk of delamination failure. The experimental and 3D simulations of "V" shape plates with different angles (60°, 90°, 120°, 150° and 180° (flat plates)) under localized blast load have been presented by Yuen et al. [21].They revealed that smaller contained angle plates divert more gas pressure accordingly less mid-point deflection of the plate. In the other work Yuen and his research group [22] analyzed the effects of orientation of blast loading onto a quadrangular plate using experiments and numerical simulations. However, their research was performed in two separate part. In first part the explosive was tilted at different angles (0°, 15°, 30° and 45°) with respect to the target plate and in other part the target plate was tilted at two different angles (15°and 45°) with respect to the explosive. Each two configuration show that tilting the explosive charge or the target plate reduced damage to the target plate. On the other hand, part of the blast load conducted onto the target plate was deflected with increasing angle of tilt; the maximum deflection of the plate was reduced. In the other study 3D numerical modeling using the finite element (FE) code ABAQUS/Explicit presented by Markose et al. [23] and the maximum central deflection, impulse transmitted and damage mode of "V" shaped plates was obtained. Chennamsetty et al. [24] proposed the experimental and numerical analysis of Hastelloy® X plates under oblique shocks. Their results demonstrated that at oblique shocked samples, the deformation start from the edge nearer to the muzzle. Adhikary et al. [25] conducted the effect of cylindrical charge orientation on the response of high strength concrete panels subject to blast loading. They considered two orientations of the cylindrical charge with respect to target panel. Their results showed that the rebar fracture was occurred when axis of the cylindrical charge oriented perpendicular to the longitudinal axis of panels whereas only a few minor cracks were observed when axis of the cylindrical charge oriented perpendicular to the longitudinal axis of panels.

The main objective of this paper is to investigate dynamic response of trapezoidal corrugated core sandwich panels under oblique blast loading. On the other hand the results of experiments and numerical simulations performed to characterize and determine the effects of orientation of blast loading onto corrugated core sandwich panels. At experimental analysis the charge, located at shock tube in the center of the target plate, was tilted to different specified angles with respect to the target plate. It is simulation of oblique blast loading on sandwich panel at small – scale version. Numerical solution has also been done in order to obtain more information and documents for explosive orientation on the spatial distribution of loading on the corrugated sandwich structure.

2 MATERIALS AND GEOMETRY

2.1 Face sheet and trapezoidal corrugated core

The front/back face sheets and trapezoidal corrugated core were manufactured from structural steel St37 (the interface sheets were placed between the core layers). The face sheet size is 270×270 *mm* with thickness of $t_f = t_b = 1mm$. The corrugated cores were made by bending approach, has a thickness of $t_c = 0.7mm$ and the same dimensions as the face sheets (see Fig.1). Another parameters at trapezoidal unit cell are $H_C = 14mm$, $B_p = 7mm$ and $\theta = 45^\circ$. Schematic of the unit cell geometry of sandwich panels is shown in Fig.2.

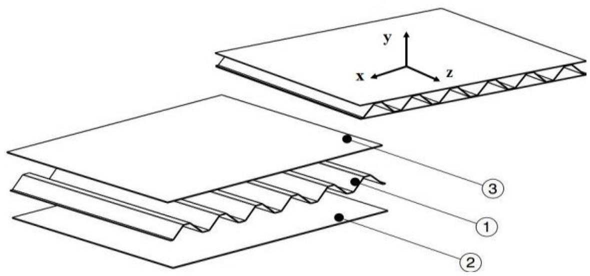

Fig.1
Schematic of the trapezoidal sandwich panel.

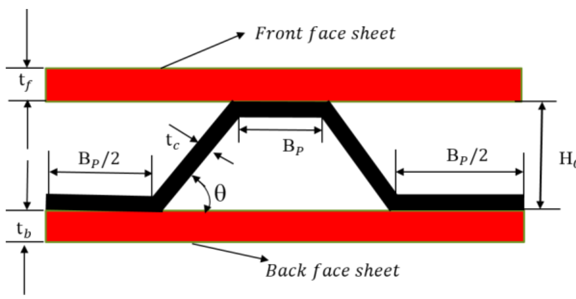

Fig.2
Schematic of the trapezoidal unit cell of sandwich panels.

3 EXPERIMANTAL SETUP

The blast test structure is placed in the blast chamber in its proper place on the fixture. The explosive charge (C4) is then placed in a special holder and covered with foam. Then, in order to prevent from moving, it is fastened to the holder with the help of adhesive tape. The electronic detonator then gently sinks into the explosive in its groove. The electric detonator wire is wiring out of the blast chamber. The detonator wire is connected to the explosion control device. Fig.3 shows experimental setup.

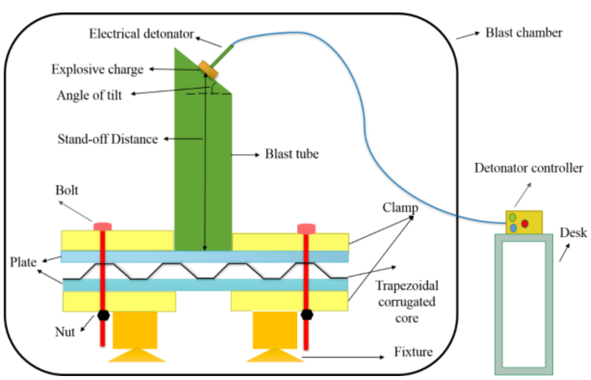

Fig.3
Configuration of full experimental setup.

3.1 Blast tubes and clamps

In this research, four types of blast tubes made of St37 with have been used, which can be considered rigid. The inner diameter of the tubes is 100 *mm* and their outer diameter is 120 *mm*. The ends of the tubes are cut by a wire-cut machine to form angles of 0, 15, 30 and 45 degrees with respect to the horizon (parallel to the target sandwich panel). The height of the tubes from the location of the charge to the target plate (stand – off distance) is 300 *mm*. These tubes are threaded from the other side to connect to the upper clamp. Fig.4 shows the mentioned tubes with the desired dimensions.

Fig.4
Four types blast tube with angle of 0°, 15°, 30°, 45°.

In order to keeping constant of sandwich panels and blast tubes two clamp made of St37 designed. The thickness of clamps is 25 *mm*, length and width of them has same dimensions as 270 *mm*. target sandwich panels was placed between clamps and closed peripherally around four edge with eight M16 bolts and nuts to the clamps. The blast tubes threads at the middle of clamps. Fig.5 represents mentioned setup.

Fig.5
Clamps, blast tube and sandwich panel.

The main purpose of this study is to investigate the effect of oblique blast loading on St37 sandwich panels. To investigate this important, four experiments were performed. The blast wave was created by the detonation of a 10 *g* cylindrical C4 explosive with a radius of 14 *mm* and a height of 10.5 *mm*.

In these experiments, for the first specimen, a blast tube with the angle of tilt equal to zero degree (parallel to the target panel) was used. At the second, third and fourth tests, were used blast tubes with the angle of tilt equal to 0°, 15°, 30°and 45° respect to the target sandwich panel, respectively. After testing of each specimen, the test kit is taken out of the blast room and the deformed panel is separated from the respective clamps and the amount of deformation of the front and back face sheets of the panel is measured and recorded by a caliper.

4 ANALYSIS OF EXPERIMENTAL RESULT

Back face sheet of the sandwich structures are deformed from a flat profile to a dome-shape geometry in all tests. (See Fig. 6) This indicates that the explosive charge is applied uniformly to the panel surface. Also, trapezoidal cells of the core are engraved on the dome-shaped area after the blast wave hits. It can be seen in Fig. 6.

Fig.6
Sandwich panels after explosion.

As can be seen in the results of Table 1, the maximum transverse deflection of the front and back face sheets (maximum damage) of the sandwich panel when occurs that the explosive charge is parallel to the target sandwich panel. On the other hand, the angle of tilt of explosive is 0°. The minimum transverse deflection also occurs when the explosive is at a 45° respect to the target sandwich panel. In other words, it can be clearly seen that by increasing the angle of tilt of explosive from 0° up to 45° respect to the target sandwich panel, the maximum transverse deflection of the front and back sheet face decreases. These results are due to the fact that when the angle of tilt increases respect to the target panel, the wave forehead meets the shock tube wall sooner and absorbs more energy. Also, by observing the results, it can be observed that the amount of back face deflection at angles of tilt 15°, 30° and 45° respect to the case of 0°, 4.68%, 5.86% and 9.77% decreases respectively. For the front face sheet the maximum deflection, 1.21%, 2.66% and 8.71% reduces.

Table 1
Summary of experimental results.

Configuration	Angle of tilt of charge (°)	Sandwich panel no.	Maximum front face deflection(*mm*)	Maximum back face deflection(*mm*)
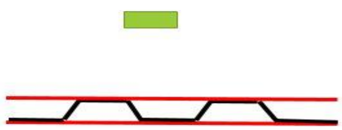	0	10R010	20.65	12.80
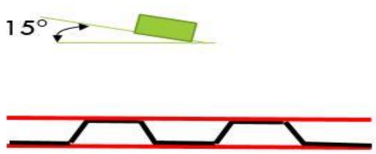	15	15R010	20.40	12.20
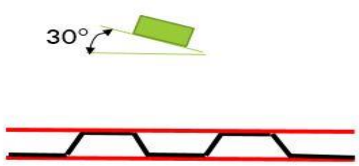	30	30R010	20.10	12.05
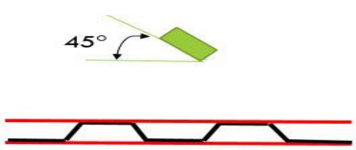	45	45R010	18.85	11.55

5 NUMERICAL SIMULATION

5.1 Coupled eulerian-lagrangian approach

For describe the deformation of a volumetric element as a function of time in solid and fluid mechanics, the Lagrangian and Eulerian approaches are presented respectively [26]. In the Lagrangian prediction, the nodes of Lagrangian element move with the material. In this situation, the interface between the two parts is precisely traced and recognized. In Eulerian description materials can transfer freely through the Eulerian domain. Therefore, Eulerian mesh remains undistorted which can track the motion of material in the Eulerian domain. This is one of the most important advantages of this method. Coupled Eulerian-Lagrangian approach allows Eulerian and Lagrangian material interact in one model [27-30]. Contact between them is modeled using a general contact. In this work the explosive and interface environment (air) are simulated as separate bodies in Eulerian domain. Eulerian elements is completely filled with them which are assigned using Eulerian volume fraction in Abaqus software. Fig.7 represents simulated set – up using CEL method.

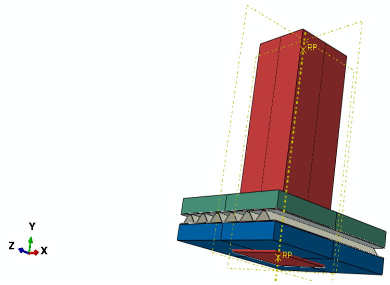

Fig.7
Simulated model with Eulerian environment.

The surrounding air was simulated as an ideal gas based on state specified at Eq. (1) as follow [14]:

$$P = (\gamma - 1)\rho e \quad \text{where } \gamma = 1 + \left(\frac{R}{C_v}\right), \; e = C_v T \tag{1}$$

where ρ is the gas density, γ is the adiabatic component, C_v is the specific heat at constant volume, R is the global gas constant, e is internal energy, T, P are the gas temperature and pressure respectively. The air parameter are listed at Table 2.

Table 2
Material properties for air (as an ideal gas) [14], [31].

$\rho(Kg/m^3)$	*R (J/kg K)*	*T(K)*	γ	C_v *(KJ/Kg K)*	*Ambient pressure(Mpa)*	*e (KJ/Kg)*
1.225	*287.058*	*288.8*	*1.4*	*0.718*	*0.101325*	2.068×10^5

The Jonson – Wilkins – Lee (JWL) Equation of state was employed to model the detonation of C4 as following equation [18]:

$$P = A\left(1 - \left(\frac{\omega}{R_1 V}\right)\right)e^{-R_1 V} + B\left(1 - \left(\frac{\omega}{R_2 V}\right)\right)e^{-R_2 V} + \frac{\omega E}{V} \tag{2}$$

In Eq. (2) A, B, R_1, R_2 and ω are material constants that related to the type of explosive. P is the blast pressure and V is the relative volume and E is the specific internal energy of explosive. Table 3 represent the value of JWL equation of state as follow:

Table 3
Material properties for C4 [31].

Density *(kg/m³)*	DetonationWawe speed*(m/s)*	*A(Gpa)*	*B(Gpa)*	R_1	R_2	ω	E_m*(MJ/kg)*
1601	8193	609.8	12.95	4.5	1.4	0.25	5.621

The Johnson Cook (JC) strength model was specified to simulate the strength properties of St37 sandwich panel which presents the flow stress as a function of equivalent plastic strain, temperature and strain rate as follow [32-33]:

$$\bar{\sigma} = \left[A + B\left(\bar{\varepsilon}^{p1}\right)^n\right]\left[1 + C\ln\left(\frac{\dot{\bar{\varepsilon}}^{p1}}{\dot{\varepsilon}_0}\right)\right]\left[1 - \left(\frac{T - T_{room}}{T_{melt} - T_{room}}\right)^m\right] \tag{3}$$

In Eq. (3) A, B, C, n, m and $\dot{\varepsilon}_0$ are the JC parameters that listed at Table 4 for steel ST37. $\bar{\sigma}$ is the von Mises flow stress, $\bar{\varepsilon}^{p1}$ is the equivalent plastic strain, $\dot{\bar{\varepsilon}}^{p1}$ is the equivalent plastic strain rate. T, T_{room} and T_{melt} are the material temperature, room temperature and melting temperature of the material respectively.

Table 4
Material properties and JC parameters for steel St37 [34].

T_{room} *(K)*	T_{melt} *(K)*	$\dot{\varepsilon}_0$ *(1/s)*	*A(Mpa)*	*B(Mpa)*	*C(Mpa)*	*m*	*N*
298	1811	1.00	350	789	0.022	1.00	0.830

For simulation of the fracture behavior of the material in the sandwich panels the JC failure model is expressed as Eq. (4) [35]. In which σ_m is the hydrostatic pressure and D_1 to D_5 are the damage model constants that listed in Table 5.

$$\bar{\varepsilon}_D^{p1} = \left[D_1 + D_2 \exp\left(\frac{\sigma_m}{\bar{\sigma}}\right)\right]\left[1 + D_4 \ln\left(\frac{\dot{\bar{\varepsilon}}^{p1}}{\dot{\varepsilon}_0}\right)\right]\left[1 + D_5\left(\frac{T - T_{room}}{T_{melt} - T_{room}}\right)\right] \tag{4}$$

Table 5
JC damage model constants for steel St37 [34].

D_1	D_2	D_3	D_4	*D5*
0.05	3.44	-2.12	0.002	0.61

For description damage of an element the linear evaluation procedure is used. It can be illustrated in damage low as below:

$$Damage = \sum \frac{\Delta\varepsilon}{\varepsilon_f} \qquad 0 < Damage < 1 \tag{5}$$

In Eq. (5) $\Delta\varepsilon$ is the equivalent plastic strain increment and ε_f is the equivalent fracture strain.

6 COMPARISION OF NUMERICAL AND EXPERIMANTAL RESULT

Fig.8 demonstrates numerical and experimental solution results for mid-point deflection of the front and back face sheets of the sandwich panel. As it is clear from the results, there is a good validation between the numerical solution and experimental results. Numerical results also indicates that with increasing the amount of angle of tilt of charge from 0° up to 45° the mid-point deflection decreases. Fig.9 and Fig.10 also show the qualitative profile of the back face deflection in *z* and *x* direction respectively for the experimental and numerical solution at angle of 15°. The numerical simulation results show a similarity with experimental studies and there is no significant difference between them.

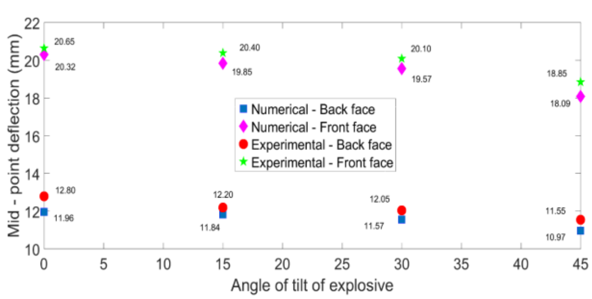

Fig.8
Comparison between central numerical and experimental of back face sheet deflection.

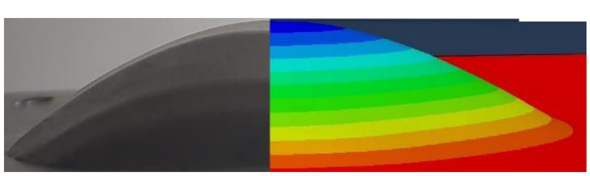

Fig.9
Displacement profile in z direction for 15°.

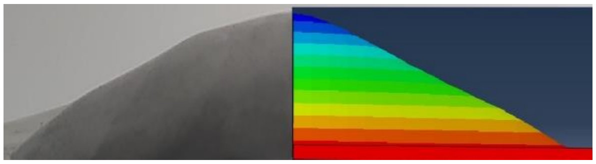

Fig.10
Displacement profile in x direction for 15°.

7 NUMERICAL RESULTS

The distribution of displacement versus distance from back face sheet center in *x* and *z* direction of sandwich panels illustrated in Fig.11 and Fig.12. The maximum deformation is at the midpoint of the sheet and the displacements decrease with distance from it. At the *z* direction, deformation profile is completely dome-shaped while the profile in the *x* direction is almost conical. This is because that core resistance is greater in the *x* direction than in *z* direction. It is evident from Fig.11 that in the middle part towards the center of the curves, a concavity has been created. Radius of this concavity increases with increasing the angle of tilt of explosive. Also due to passing through the region of regular reflection of the blast wave to the Mach stem region, the amount displacement at the angle of 45 degrees is significantly reduced compared to other angles.

In explosive loads, when the incident wave hits the surface of the sheet, a regular reflection wave will be created up to a certain angle. Unlike the sound wave, the angle of reflection will not be equal to the angle of incident. By exceeding the mentioned angle, regular reflection will not occur. Reflected wave coalesces with the incoming incident wave and forms the Mach Stem. The Mach stem is usually initiated for angles greater than 40 degrees to detonate in air [36].

A comparison of the Johnson-Cook damage parameter as well as its evolution over time for the back face sheet center of sandwich panel is shown in Fig.13. As it is known, this parameter is increasing over time and is at its lowest value for a 45° angle and at its maximum value for a 0°.

As indicated in Fig.14 the increasing the mass of explosive has a significant influence on the maximum displacement of back face sheet center. It is evidence that with increasing the mass of explosive the maximum displacement decreases. It is also obvious that at larger mass of explosive, the decrease in the deformations is more pronounced with increasing angle of tilt of explosive. When the explosive was tilt respect to the angle of 0° the half of explosive goes further from target sandwich plate.

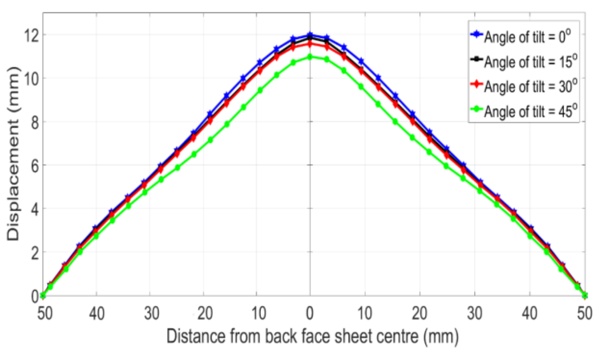

Fig.11
Distribution of displacement versus distance from back face sheet center in *x* direction.

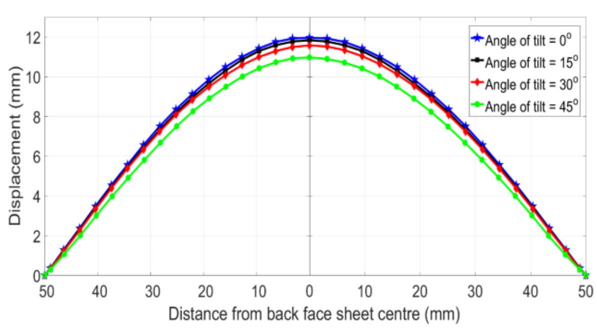

Fig.12
Distribution of displacement versus distance from back face sheet center in *z* direction.

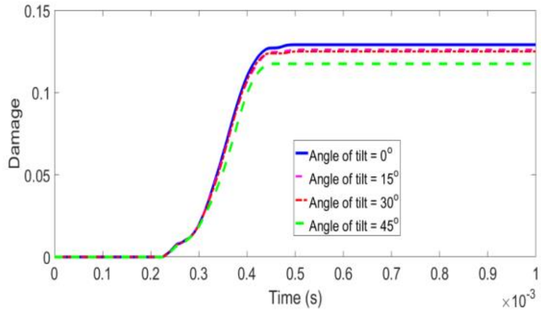

Fig.13
Comparison of the JC damage parameter versus time for back face sheet center.

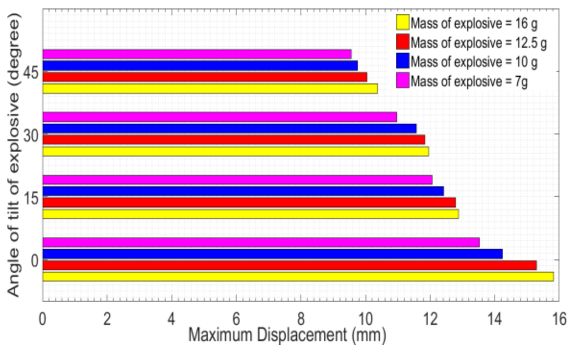

Fig.14
Effect of increasing mass of explosive on the maximum displacement of back face sheet center for different angles.

8 CONCLUSIONS

In this research, dynamic response of corrugated core sandwich panels under oblique blast loading was presented. Four experiments at the angle of tilt of explosive 0°, 15°, 30° and 45° respect to sandwich plate are performed. Using CEL approach in Abaqus commercial software numerical analysis was investigated. The effects of angle of tilt of explosive on the maximum displacement of back face sheet center in x and z directions, Johnson-Cook damage parameter and increasing mass of explosive were taken into account. The results of this study are listed as follows:

- It is seen that the amount of back face deflection at angles of tilt 15°, 30° and 45° respect to the case of 0°, 4.68%, 5.86% and 9.77% decreases respectively. For the front face sheet the maximum deflection, 1.21%, 2.66% and 8.71% reduces. Because of passing through the region of regular reflection to the Mach stem region (irregular reflection), the amount displacement at the angle of 45 degrees is significantly reduced compared to other angles.
- It is found that at the z direction, deformation profile is completely dome-shaped while the profile in the x direction is almost conical. This is because that core resistance is greater in the x direction than in z direction
- JC parameter is increasing over time and is at its lowest value for a 45° angle and at its maximum value for a 0°.
- It is seen that with increasing the mass of explosive the maximum displacement decreases. It is also obvious that at larger mass of explosive, the decrease in the deformations is more pronounced with increasing angle of tilt of explosive.

REFERENCES

[1] Anderson Jr C.E., Behner T., Weiss C.E., 2011, Mine blast loading experiments, *International Journal of Impact Engineering* **38**(8-9): 697-706.

[2] Gurumurthy G., 2008, *Blast Mitigation Strategies for Vehicles Using Shape Optimization Methods*, Thesis (S.M.) Massachusetts Institute of Technology, Computation for Design and Optimization Program.

[3] Markose A., Rao C.L., 2017, Mechanical response of V shaped plates under blast loading, *Thin-Walled Structures* **115**:12-20.

[4] Nurick G.N., Lockley J.P., 1999, Experimental investigation to evaluate the effect of the included angle of a folded "V" shape plate for blast resistance, *1st International Conference on Integrity, Reliabality and Failure*, Porto Portugal.
[5] Langdon G.S., Yuen S.C.K., Nurick G.N., Naidoo K., 2013, Some insights into the response of 'shallow V shape'structures to air blast loading, *Proceedings of the National Academy of Sciences of the United States of America* **79**(4):695-703.
[6] Li S., Li X., Wang Z., Wu G., Lu G., Zhao L., 2016, Finite element analysis of sandwich panels with stepwise graded aluminum honeycomb cores under blast loading, *Composites Part A: Applied Science and Manufacturing* **80**:1-12.
[7] Imbalzano G., Linforth S., Ngo T.D., Lee P.V.S.,Tran P., 2018, Blast resistance of auxetic and honeycomb sandwich panels: Comparisons and parametric designs, *Composite Structures* **183**: 242-261.
[8] Liu X., Tian X., Lu T.J., Zhou D., Liang B., 2012, Blast resistance of sandwich-walled hollow cylinders with graded metallic foam cores, *Composite Structures* **94**(8): 2485-2493.
[9] Dharmasena K.P., Wadley H.N., Xue Z., Hutchinson J.W., 2008, Mechanical response of metallic honeycomb sandwich panel structures to high-intensity dynamic loading, *International Journal of Impact Engineering* **35**(9):1063-1074.
[10] Qi C., Yang S., Yang L.J., Han S.H., Lu Z.H., 2014, Dynamic response and optimal design of curved metallic sandwich panels under blast loading, *The Scientific World Journal* **2014**: 853681.
[11] Jing L., Wang Z., Zhao L., 2013, Dynamic response of cylindrical sandwich shells with metallic foam cores under blast loading—numerical simulations, *Composite Structures* **99**: 213-223.
[12] Sun G., Zhang J., Li S., Fang J., Wang E., Li Q., 2019, Dynamic response of sandwich panel with hierarchical honeycomb cores subject to blast loading, *Thin-Walled Structures* **142**: 499-515.
[13] Cai S., Zhang P., Dai W., Cheng Y., Liu J., 2021, Multi-objective optimization for designing metallic corrugated core sandwich panels under air blast loading, *Journal of Sandwich Structures & Materials* **23**(4):1192-1220.
[14] Zhang P., Cheng Y., Liu J., 2014, Numerical analysis of dynamic response of corrugated core sandwich panels subjected to near-field air blast loading, *Shock and Vibration* **2014**: 180674.
[15] Zhang P., Cheng Y., Liu J., Wang C., Hou H., Li Y., 2015, Experimental and numerical investigations on laser-welded corrugated-core sandwich panels subjected to air blast loading, *Marine Structures* **40**: 225-246.
[16] Cheng Y., Liu M., Zhang P., Xiao W., Zhang C., Liu J., Hou H., 2018, The effects of foam filling on the dynamic response of metallic corrugated core sandwich panel under air blast loading–Experimental investigations, *International Journal of Mechanical Sciences* **145**: 378-388.
[17] Zhang P., Cheng Y., Liu J., Li Y., Zhang C., Hou H., Wang C., 2016, Experimental study on the dynamic response of foam-filled corrugated core sandwich panels subjected to air blast loading, *Composites Part B: Engineering* **105**: 67-81.
[18] Li S., Li X., Wang Z., Wu G., Lu G., Zhao L., 2017, Sandwich panels with layered graded aluminum honeycomb cores under blast loading, *Composite Structures* **173**: 242-254.
[19] Zhang P., Liu J., Cheng Y., Hou H., Wang C., Li Y., 2015, Dynamic response of metallic trapezoidal corrugated-core sandwich panels subjected to air blast loading–An experimental study, *Materials & Design* **65**: 221-230.
[20] Zhou T., Zhang P., Xiao W., Liu J., Cheng Y., 2019, Experimental investigation on the performance of PVC foam core sandwich panels under air blast loading, *Composite Structures* **226**:111081.
[21] Yuen S.C.K., Langdon G.S., Nurick G.N., Pickering E.G., Balden V.H., 2012, Response of V-shape plates to localised blast load: Experiments and numerical simulation, *International Journal of Impact Engineering* **46**: 97-109.
[22] Yuen S.C.K., Butler A., Bornstein H., Cholet A., 2018, The influence of orientation of blast loading on quadrangular plates, *Thin-Walled Structures* **131**: 827-837.
[23] Markose A., Rao C.L., 2017, Mechanical response of V shaped plates under blast loading, *Thin-Walled Structures* **115**: 12-20.
[24] Chennamsetty A.R.K., LeBlanc J., Abotula S., Parrikar P.N., Shukla A., 2015, Dynamic response of Hastelloy® X plates under oblique shocks: Experimental and numerical studies, *International Journal of Impact Engineering* **85**: 97-109.
[25] Adhikary S.D., Chandra L.R., Christian A., Ong K.C.G., 2017, Influence of cylindrical charge orientation on the blast response of high strength concrete panels, *Engineering Structures* **149**: 35-49.
[26] Qiu G., Henke S., Grabe J., 2011, Application of a Coupled Eulerian–Lagrangian approach on geomechanical problems involving large deformations, *Computers and Geotechnics* **38**(1): 30-39.
[27] Hamann T., Qiu G., Grabe J., 2015, Application of a Coupled Eulerian–Lagrangian approach on pile installation problems under partially drained conditions, *Computers and Geotechnics* **63**: 279-290.
[28] Zaidi A.M.A., Koslan F.S., Othman Z., Manar G., 2013, Appropriate coupling solvers for the numerical simulation of rolled homogeneous armor plate response subjected to blast loading, *Advances in Mechanical Engineering* **5**: 637564.
[29] Birnbaum N.K., Francis N.J., Gerber B.I., 1999, Coupled techniques for the simulation of fluid-structure and impact problems, *Computer Assisted Mechanics and Engineering Sciences* **6**(3/4): 295-312.
[30] Nasiri S., Sadegh-Yazdi M., Mousavi S.M., Ziya-Shamami M., Mostofi T.M., 2022, Repeated underwater explosive forming: Experimental investigation and numerical modeling based on coupled Eulerian–Lagrangian approach, *Thin-Walled Structures* **172**:108860.
[31] Henchie T.F., Yuen S.C.K., Nurick G.N., Ranwaha N., Balden V.H., 2014, The response of circular plates to repeated uniform blast loads: An experimental and numerical study, *International Journal of Impact Engineering* **74**: 36-45.

[32] Johnson G.R., 1983, A constitutive model and data for materials subjected to large strains, high strain rates, and high temperatures, *Proceedings Seventh International Symposium on Ballistics, Hague, Netherlands*.
[33] Haghgoo M., Babaei H., 2021, 2D Numerical simulation of the nonlinear deformation of thin plate under gaseous mixture detonation axisymmetric loading, *Modares Mechanical Engineering* **21**(11): 729-742.
[34] Öztürk G., 2010, *Numerical and Experimental Investigation of Perforation of ST-37 Steel Plates by Oblique Impact*, Master's Thesis, Middle East Technical University.
[35] Rezasefat M., Mostofi T.M., Ozbakkaloglu T., 2019, Repeated localized impulsive loading on monolithic and multi-layered metallic plates, *Thin-Walled Structures* **144**:106332.
[36] Rigby S.E., Knighton R., Clarke S.D., Tyas A., 2020, Reflected near-field blast pressure measurements using high speed video, *Experimental Mechanics* **60**(7): 875-88.